Transfer ionization in fast ion-atom collisions: Four-body Born distorted-wave theory

Dževad Belkić[1] and Ivan Mančev[2]
[1]*Karolinska Institute, SE-171 76 Stockholm, Sweden*
[2]*Department of Physics, Faculty of Sciences and Mathematics, University of Niš, 18000 Niš, Serbia*
(Received 16 November 2010; published 13 January 2011)

The theory of transfer ionization in fast ion-atom collisions is investigated within the four-body distorted-wave formalism. The four-body Born distorted-wave (BDW-4B) method, which was originally introduced for double electron capture, is presently extended to transfer ionization. In the entrance and exit channel, the BDW-4B method coincides with the four-body versions of the boundary-corrected first Born and the continuum distorted wave approximations, respectively. An illustrative application of the present method is performed for the previously most studied case of transfer ionization in proton-helium collisions at intermediate and high energies (0.3–10 MeV). The obtained total cross sections are compared with all the available experimental data. Overall, very good agreement is found, particularly at high impact energies that are within the expected region of validity of the BDW-4B approximation.

DOI: 10.1103/PhysRevA.83.012703 PACS number(s): 34.70.+e, 82.30.Fi, 03.65.Nk

I. INTRODUCTION

Two-electron transitions in four-body fast ion-atom collisions have been extensively studied in the last two decades both theoretically and experimentally (see, e.g., the most recent reviews and books with the references cited therein [1–4]). This includes transfer ionization as a collision between a nucleus as a projectile and a multi-electron target from which one electron is captured and the other ionized. Transfer ionization still remains one of the most challenging collisional processes with two active electrons even in the simplest case, which involves heliumlike targets. This scattering phenomenon has opened interesting and fruitful discussions about different scattering mechanisms, including the role of static as well as dynamic electron correlations. In spite of a markedly rapid decrease of the total cross section, much attention in the past literature has been devoted to transfer ionization at relatively high impact energies.

The first systematic measurements of total cross sections for transfer ionization of He by fast H^+, He^{2+}, and Li^{3+} ions were made by Shah and Gilbody [5,6]. Later, Mergel *et al.* [7] measured total cross sections in H^+-He collisions at projectile energies 0.15–1.4 MeV by means of cold-target recoil-ion momentum spectroscopy (COLTRIMS). They reported the first kinematically complete experiment for transfer ionization. Using a convenient combination of high-quality ion beams that were available in the heavy-ion storage ring CRYRING with the COLTRIMS setup and a pulsed extraction system, Schmidt *et al.* [8–10] measured total cross sections for transfer ionization in the high-energy range 1.4–5.8 MeV in H^+-He collisions. Woitke *et al.* [11] and most recently Sant'Anna *et al.* [12] measured total cross sections of transfer ionization for Li^{3+}-He collisions at larger energies than those from the experiments by Shah and Gilbody [5].

Several research groups have reported on theoretical studies by focusing on total cross sections for transfer ionization. The semiclassical independent-event model (IEM) of Dunseath and Crothers [13] gave cross sections that were considerably larger than those of the corresponding experiments in collisions of H^+ and He^{2+} nuclei with a helium target. Using a coupled channel semiclassical impact parameter approximation with a traveling atomic orbital expansion and employing the independent particle model (IPM), Singhal and Lin [14] obtained results that overestimated the measured cross sections and clearly revealed the inadequacy of simple uncorrelated models to describe pure four-body problems of scattering. The IPM was also employed in Ref. [15]. A simple variant within the IPM based on the Bohr-Lindhard and the classical statistical models has been developed in Ref. [16] for transfer ionization of helium by ions A^{q+} ($q = 1$–3). Both the IEM and IPM ignore the inter-electron correlations from the outset and compute the probability for transfer ionization as a product of the individual probabilities for capture of one electron and independent ionization of the other electron. Galassi *et al.* [17] employed the IPM to compute total cross sections for transfer ionization in (H^+,He^{2+})-He collisions. In the latter study, the single particle probabilities as a function of impact parameter were computed using the continuum-distorted-wave eikonal initial state (CDW-EIS) method. Their results [17] are in better agreement with measurements than the computations of Dunseath and Crothers [13], but are still larger than the experimental values, especially for the case of H^+ impact. Using the second Born approximation, Godunov *et al.* [18] found that the allowance for static electron correlation directly determines how closely the obtained theoretical total cross sections agree with the experimental data. The latter results from the second-order computations [18] with the uncorrelated functions differ considerably from experimental data, whereas an approximate inclusion of static correlations gives noticeably better agreement with the same measurements. In the computations from Ref. [18], an additional approximation was used for the dynamic electron-electron correlation $1/|\boldsymbol{r}_1 - \boldsymbol{r}_2|$ from the perturbation potential in the exit channel via $-Z_T/r_1 + 1/|\boldsymbol{r}_1 - \boldsymbol{r}_2| \simeq -(Z_T - 1)/r_1$, where $\boldsymbol{r}_1$ and $\boldsymbol{r}_2$ are the position vectors of the electrons e_1 and e_2 relative to the target nuclear charge Z_T, respectively. The four-body continuum distorted wave (CDW-4B) method has been formulated and implemented by Belkić *et al.* [19] for He^{2+}-He collisions, resulting in very good agreement with measurements. Later on, the CDW-4B method employed by Mančev [20] was also

found to be in very good agreement with the experimental data for Li^{3+}-He collisions.

Studying the collision mechanisms for transfer ionization within differential cross sections has been the subject of numerous investigations from the experimental and theoretical standpoints [21–37]. In these examinations, transfer ionization by proton impact clearly dominates because the exit channel contains no three-body Coulomb interaction. This is due to the fact that the proton captures one electron to become a neutral hydrogen atom and, therefore, one could expect that the postcollisional interaction with the projectile system would be weak, as indeed turned out to be the case.

The present work is concerned with the extension of the four-body Born distorted wave (BDW-4B) method from its original inception for double charge exchange [38] to transfer ionization. The BDW-4B theory is a fully quantum-mechanical four-body formalism, since it explicitly considers each individual particle and all the interactions among them in the collision under investigation. This permits a systematic study of the complete dynamics of four-body scattering processes [38,39]. The BDW-4B method strictly preserves the correct boundary conditions in both collisional channels according to the principles of scattering theory [40] and the asymptotic convergence problem introduced by Dollard [41]. This amounts to an explicit inclusion of all the Coulomb distortion effects of the unperturbed channel states, with a simultaneous and consistent subtraction of the static Coulomb interactions from the perturbation potentials in the initial and final states [1–3,40–43]. Thus, in the entrance channel, the initial state is taken as being influenced only by the motion of the two heavy scattering aggregates. This yields a distortion of the initial scattering state through a logarithmic phase due to the perturbation potential from the remaining asymptotic Coulomb interaction between the projectile and the point charge of the target as a whole. In the exit channel, alongside the logarithmic phase for the motion of heavy particles, an appropriate distortion of the final state is included through the two full Coulomb wave functions for the ejected and captured electron in the field of the bare and partially screened target nuclear charge, respectively. Therefore, the BDW-4B approximation coincides with the CDW-4B [19] method in the exit channel. On the other hand, in the entrance channel, the BDW-4B method reduces to the four-body boundary-corrected first Born (CB1-4B) approximation [44]. After its formulation and implementation in the case of double charge exchange [38], the BDW-4B approximation was also successfully applied to single-electron capture by fast nuclei and hydrogenic ions from heliumlike targets [45–47].

Multiple differential cross sections for transfer ionization can undeniably yield the most detailed insight into versatile collisional mechanisms. However, when it comes to the usage of the abundant atomic databases in other neighboring fields of fundamental and applied research, total cross sections were most frequently needed. The primary reason for this is that in various applications ranging from plasma physics through thermonuclear fusion to hadron therapy in medicine, total cross sections for atomic collisional processes are the principal entries to comprehensive Monte Carlo simulation codes for reliable assessment of energy losses of multiply charged heavy ions during their passage through matter. In these stochastic simulations, total cross sections directly determine the stopping powers of heavy ions. For example, in hadron therapy, radiation doses delivered by heavy ions to the treatment site in patients are critically dependent upon the accuracy of total cross sections (and the ensuing stopping powers) for various atomic and nuclear collisions taking place in the tissue during the treatment. A detailed exposition of many essential applications of the theory of atomic collisions to hadron therapy in cancer treatment can be found in the most recent review [48]. The larger the charge of the projectile, the higher the probability for multiple electron transitions, including a combination of simultaneous formation of bound states and emission of electrons into their continua, as is actually the case in transfer ionization. Because of a widely expressed and urgent need from many different applications in interdisciplinary fields, we are concerned here with computations of mainly total cross sections for transfer ionization. For an implementation and illustration of the proposed BDW-4B method, we choose the prototype process in H^+-He collisions at impact energies $E = 0.3$–10 MeV, at which the three sets of independent experimental data are currently available.

Atomic units will be used throughout unless otherwise stated.

II. THEORY

We examine a collision in which a fully stripped projectile P of charge Z_P impinges upon a heliumlike atomic system consisting of two electrons e_1 and e_2 that are initially bound to the target nucleus T of charge Z_T. During such a collision, one electron (e_1) is captured by P into a bound state $(Z_P,e_1)_f$, whereas the other electron (e_2) is simultaneously ionized:

$$Z_P + (Z_T;e_1,e_2)_i \longrightarrow (Z_P,e_1)_f + Z_T + e_2(\boldsymbol{\kappa}). \tag{1}$$

Here, $\boldsymbol{\kappa}$ represents the momentum vector of the ejected electron e_2 with respect to its parent nucleus T. In Eq. (1), the small parentheses symbolize the bound states, whereas the subscripts i and f are the collective labels for the sets of the usual quantum numbers. Thus, e.g., for the hydrogenlike system $(Z_P,e_1)_f$, we have $f \equiv \{n_f,\ell_f,m_f\}$, where n_f, ℓ_f, and m_f are the principal, angular, and magnetic quantum numbers, respectively. Let $\boldsymbol{s}_k$ and $\boldsymbol{x}_k$ be the position vectors of e_k ($k = 1,2$) relative to the nuclear charge Z_P and Z_T, respectively. Further, let $\boldsymbol{R}$ denote the position vector of Z_P with respect to Z_T. The vector of the distance between the two electrons e_1 and e_2 is labeled $\boldsymbol{r}_{12}$, where $\boldsymbol{r}_{12} = \boldsymbol{x}_1 - \boldsymbol{x}_2 = \boldsymbol{s}_1 - \boldsymbol{s}_2$. In the quantum-mechanical four-body distorted wave formalism [1–3], the post form of the transition amplitude for process (1) is:

$$T_{if}^{+} = \langle \chi_f^{-} | U_f | \Phi_i^{+} \rangle. \tag{2}$$

The initial wave function Φ_i^+ in the entrance channel with the asymptotically correct boundary condition can be written as follows:

$$\Phi_i^{+} = \varphi_i(\boldsymbol{x}_1,\boldsymbol{x}_2) e^{i\boldsymbol{k}_i\cdot\boldsymbol{r}_i + i\nu_i \ln(vR - \boldsymbol{v}\cdot\boldsymbol{R})}, \tag{3}$$

where vector $\boldsymbol{r}_i$ is the relative vector of Z_P with respect to the center of mass of $(Z_T;e_1,e_2)_i$. Function $\varphi_i(\boldsymbol{x}_1,\boldsymbol{x}_2)$ represents the two-electron bound-state wave function of the

atomic system $(Z_T;e_1,e_2)_i$, whereas $\boldsymbol{k}_i$ is the initial wave vector, $\nu_i = Z_P(Z_T-2)/v$, and $\boldsymbol{v}$ is the impact velocity vector. The unperturbed part $\varphi_i(\boldsymbol{x}_1,\boldsymbol{x}_2)e^{i\boldsymbol{k}_i\cdot\boldsymbol{r}_i}$ of the initial state Φ_i^+ from Eq. (3) is distorted by $e^{i\nu_i \ln(vR-v\cdot R)}$ even at infinite separations between the two scattering aggregates. This is due to the presence of the asymptotic Coulomb repulsive potential, $V_i^\infty = Z_P(Z_T-2)/R$, between the projectile and the screened target nucleus of point charge Z_T-2. Here, V_i^∞ is the asymptotic limit of the perturbation potential V_i in the entrance channel, where $V_i = Z_P Z_T/R - Z_P/s_1 - Z_P/s_2 \longrightarrow Z_P(Z_T-2)/R$ as $R\to\infty$, in which case we also have $s_k\to\infty\,(k=1,2)$.

In the BDW-4B theory, the distorting potential U_f and the distorted wave function χ_f^- are chosen according to

$$U_f = Z_P\left(\frac{1}{R}-\frac{1}{s_2}\right)+\left(\frac{1}{r_{12}}-\frac{1}{x_1}\right)-\boldsymbol{\nabla}_{s_1}\ln\varphi_f\cdot\boldsymbol{\nabla}_{x_1}, \quad (4)$$

$$\begin{aligned}\chi_f^- &= N^-(\zeta)N^-(\nu_T)\phi_f\varphi_f(\boldsymbol{s}_1)e^{-i\boldsymbol{k}_f\cdot\boldsymbol{r}_f-iv_f\ln(vR+v\cdot R)}\\ &\times {}_1F_1(-i\zeta,1,-ipx_2-i\boldsymbol{p}\cdot\boldsymbol{x}_2)\\ &\times {}_1F_1(-i\nu_T,1,-ivx_1-i\boldsymbol{v}\cdot\boldsymbol{x}_1).\end{aligned} \quad (5)$$

Here, $\phi_f = (2\pi)^{-3/2}e^{i\boldsymbol{\kappa}\cdot\boldsymbol{x}_2}$, $\varphi_f(\boldsymbol{s}_1)$ is a hydrogenlike wave function of $(Z_P,e_1)_f$, $\boldsymbol{r}_f$ is the position vector of T with respect to the center of mass of $(Z_P,e_1)_f+e_2$ in the exit channel, $\boldsymbol{k}_f$ is the final wave vector, $N^-(\zeta)=\Gamma(1+i\zeta)e^{\pi\zeta/2}$, and $N^-(\nu_T)=\Gamma(1+i\nu_T)e^{\pi\nu_T/2}$, where $\nu_T=(Z_T-1)/v$, $\nu_f=Z_P(Z_T-1)/v$, $\zeta=Z_T/p$, and $\boldsymbol{p}=\boldsymbol{\kappa}+\boldsymbol{v}$. The symbol ${}_1F_1(a,b,z)$ stands for the Kummer confluent hypergeometric function. By means of the well-known asymptotic forms of ${}_1F_1(a,b,z)$, it is readily seen that the wave function χ_f^- obeys the correct boundary conditions in the asymptotic region $(R\to\infty)$ [1–3].

Using Eqs. (3), (4), and (5), the expression for the transition amplitude T_{if}^+ becomes

$$\begin{aligned}T_{if}^+ &= N^{-*}\iiint d\boldsymbol{R}\,d\boldsymbol{x}_1\,d\boldsymbol{x}_2 e^{i\boldsymbol{\alpha}\cdot\boldsymbol{s}_1+i\boldsymbol{\beta}\cdot\boldsymbol{x}_1-i\boldsymbol{\kappa}\cdot\boldsymbol{x}_2}\mathcal{L}(R)\varphi_i(\boldsymbol{x}_1,\boldsymbol{x}_2)\\ &\times {}_1F_1(i\zeta,1,ipx_2+i\boldsymbol{p}\cdot\boldsymbol{x}_2)\{[Z_P(1/R-1/s_2)\\ &+(1/r_{12}-1/x_1)]\,{}_1F_1(i\nu_T,1,ivx_1+i\boldsymbol{v}\cdot\boldsymbol{x}_1)\varphi_f^*(\boldsymbol{s}_1)\\ &-\boldsymbol{\nabla}_{s_1}\varphi_f^*(\boldsymbol{s}_1)\cdot\boldsymbol{\nabla}_{x_1}\,{}_1F_1(i\nu_T,1,ivx_1+i\boldsymbol{v}\cdot\boldsymbol{x}_1)\},\end{aligned} \quad (6)$$

where $N^- = (2\pi)^{-3/2}N^-(\nu_T)N^-(\zeta)$. In Eq. (6), the auxiliary function $\mathcal{L}(R)$ represents the product of the two logarithmic Coulomb factors $e^{i\nu_i\ln(vR-v\cdot R)}$ and $e^{iv_f\ln(vR+v\cdot R)}$. Function $\mathcal{L}(R)$ can advantageously be reduced to the following expression with only one remaining logarithmic Coulomb phase factor:

$$\mathcal{L}(R) = e^{i\nu_i\ln(vR-v\cdot R)+iv_f\ln(vR+v\cdot R)} = (\rho v)^{2i\nu_i}(vR+\boldsymbol{v}\cdot\boldsymbol{R})^{i\xi}, \quad (7)$$

where $\xi = Z_P/v$ and $\boldsymbol{\rho}$ is the projection of vector $\boldsymbol{R}$ onto the XOY plane ($\boldsymbol{\rho}=\boldsymbol{R}-\boldsymbol{Z}$, $\boldsymbol{\rho}\cdot\boldsymbol{Z}=0$). Here, $\boldsymbol{Z}$ is the vectorial component of $\boldsymbol{R}$ in the direction of the the Z axis. The multiplying term $(\rho v)^{2i\nu_i}$ does not contribute to the total cross section and, therefore, can be dropped from the transition amplitudes [43]. In addition to this significant simplification, we have also used the eikonal hypothesis ($\widehat{\boldsymbol{k}}_f\approx\widehat{\boldsymbol{k}}_i$), since the small-angle limit is amply justified for heavy particles, and this yields

$$\boldsymbol{k}_i\cdot\boldsymbol{r}_i+\boldsymbol{k}_f\cdot\boldsymbol{r}_f\approx\boldsymbol{\alpha}\cdot\boldsymbol{s}_1+\boldsymbol{\beta}\cdot\boldsymbol{x}_1, \quad (8)$$

where $\boldsymbol{\alpha}$ and $\boldsymbol{\beta}$ are the two momentum transfers introduced by

$$\begin{aligned}\boldsymbol{\alpha} &= \boldsymbol{\eta}-\left(\frac{v}{2}-\frac{E_i-E_f-E_\kappa}{v}\right)\widehat{\boldsymbol{v}},\\ \boldsymbol{\beta} &= -\boldsymbol{\eta}-\left(\frac{v}{2}+\frac{E_i-E_f-E_\kappa}{v}\right)\widehat{\boldsymbol{v}},\end{aligned} \quad (9)$$

with $\boldsymbol{v}=(0,0,v)$ and $\boldsymbol{\eta}\cdot\boldsymbol{v}=0$. The quantity E_i is the initial electronic binding energy of $(Z_T;e_1,e_2)_i$, whereas the final discrete and continuous energies of e_1 and e_2 are $E_f=-Z_P^2/(2n_f^2)$ and $E_\kappa=\kappa^2/2$, respectively. The transverse component of the change in the relative linear momentum of a heavy particle is denoted by $\boldsymbol{\eta}=(\eta\cos\phi_\eta,\eta\sin\phi_\eta,0)$. By inspection, it is at once seen that the BDW-4B method exactly coincides with the CDW-4B method [19] in the exit channel, and with the CB1-4B approximation [44] in the entrance channel. Therefore, the BDW-4B method preserves the correct boundary conditions in both scattering channels for transfer ionization, as was originally the case for double electron capture [38,39] within the same theoretical framework. The initial state of $(Z_T;e_1,e_2)_i$ is presently taken to be the ground state $(i=1s^2)$ and, as such, is described by the simplest Hylleraas-type wave function [49] without static correlations $\varphi_i(\boldsymbol{x}_1,\boldsymbol{x}_2)=\varphi_b(\boldsymbol{x}_1)\varphi_b(\boldsymbol{x}_2)$, where $\varphi_b(\boldsymbol{r})=N_b\exp(-br)$, $N_b=(b^3/\pi)^{1/2}$, and b is the Slater-type effective nuclear charge $(b=Z_T-0.3125)$.

Thus far, experience with computations of total cross sections has shown that for different single- and double-electron transitions [1–3], the terms $V_{P,s_2}\equiv Z_P(1/R-1/s_2)$ and $V_{12,1}\equiv(1/r_{12}-1/x_1)$ give contributions of varying significance, depending on the kind of collision examined. Regarding the complexity of the analysis, one is faced with a considerably increased computational demand when the perturbation potentials V_{P,s_2} and $V_{12,1}$ are explicitly incorporated into the transition amplitude of any approximation, including the BDW-4B method. This is due to the two additional three-dimensional quadratures that arise from the Fourier transform for V_{P,s_2} and $V_{12,1}$. Because of this circumstance, the present application of the BDW-4B method to transfer ionization will simplify the distorting perturbation U_f from Eq. (4) to retain only the gradient-gradient term $(\boldsymbol{\nabla}\cdot\boldsymbol{\nabla})$, as was done in the majority of previous computations, e.g., in the CDW method for heliumlike targets [1,2,40,43]. In such a case, the transition amplitude is reduced to the following expression for a particular case of the final ground state $1s\,(f=\{n_f,\ell_f,m_f\}=\{1,0,0\})$ of the hydrogenlike system $(Z_P,e_1)_f$:

$$T_{if}^+ = \frac{1}{\sqrt{\pi}}N^{-*}Z_P^{3/2}N_b^2\int d\boldsymbol{R}(vR+\boldsymbol{v}\cdot\boldsymbol{R})^{i\xi}e^{-i\boldsymbol{\alpha}\cdot\boldsymbol{R}}\mathcal{D}_1\mathcal{D}_2, \quad (10)$$

where

$$\begin{aligned}\mathcal{D}_1 &= \int d\boldsymbol{x}_1 e^{-iv\cdot x_1-bx_1}\left[\boldsymbol{\nabla}_{s_1}e^{-Z_P s_1}\right]\\ &\times[\boldsymbol{\nabla}_{x_1}\,{}_1F_1(i\nu_T,1,ivx_1+i\boldsymbol{v}\cdot\boldsymbol{x}_1)],\end{aligned} \quad (11)$$

$$\mathcal{D}_2 = \int d\boldsymbol{x}_2 e^{-i\boldsymbol{\kappa}\cdot\boldsymbol{x}_2-bx_2}\,{}_1F_1(i\zeta,1,ipx_2+i\boldsymbol{p}\cdot\boldsymbol{x}_2). \quad (12)$$

Using the following standard real integral for a convenient representation of the confluent hypergeometric function [50] in Eq. (11):

$$ {}_1F_1(i\nu_T,1,iv x_1 + i\boldsymbol{v}\cdot\boldsymbol{x}_1) = \frac{1}{\Gamma(i\nu_T)\Gamma(1-i\nu_T)}\int_0^1 dt_1 f_T(t_1) e^{i(vx_1+v\cdot x_1)t_1}, \quad (13)$$

where $f_T(t_1) = t_1^{i\nu_T-1}(1-t_1)^{-i\nu_T}$, the integral $\mathcal{D}_1$ becomes

$$ \mathcal{D}_1 = \frac{1}{\Gamma(i\nu_T)\Gamma(1-i\nu_T)}\int_0^1 dt_1 f_T(t_1)\mathcal{F}_1(\boldsymbol{R}), \quad (14)$$

where

$$ \mathcal{F}_1(\boldsymbol{R}) = \int d\boldsymbol{x}_1 e^{-iv\cdot x_1 - bx_1}\left[\nabla_{s_1} e^{-Z_P s_1}\right]\cdot\left[\nabla_{x_1}\Omega(\boldsymbol{x}_1)\right], \quad (15)$$

with $\Omega(\boldsymbol{x}_1) = e^{i(vx_1+v\cdot x_1)t_1}$. Integral $\mathcal{F}_1(\boldsymbol{R})$ can be analytically reduced to a one-dimensional integral following Ref. [38], as outlined in the present appendix. With this result, the original nine-dimensional integral for the matrix element T_{if}^+ is reduced to a two-dimensional numerical quadrature with real variables.

The triple differential cross sections for simultaneous transfer and ionization can be obtained from the expression

$$ Q_{if}^+(\boldsymbol{\kappa}) \equiv \frac{d^3Q_{if}^+}{d\boldsymbol{\kappa}} = \frac{1}{4\pi^2 v^2}\int d\boldsymbol{\eta}|T_{if}^+(\boldsymbol{\eta})|^2. \quad (16)$$

Here, the transition amplitude $T_{if}^+(\boldsymbol{\eta})$ is independent of the azimuthal angle ϕ_η, i.e., $T_{if}^+(\boldsymbol{\eta}) = T_{if}^+(\eta)$. Therefore, the integration over ϕ_η can be done analytically to yield

$$ Q_{if}^+(\boldsymbol{\kappa}) = \frac{1}{2\pi v^2}\int_0^\infty d\eta\,\eta|T_{if}^+(\eta)|^2. \quad (17)$$

The total cross section is introduced as a triple integration over the momentum $\boldsymbol{\kappa}$ of the ejected electron, where $\boldsymbol{\kappa} = (\kappa\sin\theta_\kappa\cos\phi_\kappa, \kappa\sin\theta_\kappa\sin\phi_\kappa, \kappa\cos\theta_\kappa)$:

$$ Q_{if}^+(\pi a_0^2) \equiv \int d\boldsymbol{\kappa}\, Q_{if}^+(\boldsymbol{\kappa}) = \int_0^\infty d\kappa\kappa^2\int_0^\pi d\theta_\kappa\sin\theta_\kappa \times \int_0^{2\pi} d\phi_\kappa\, Q_{if}^+(\boldsymbol{\kappa}). \quad (18)$$

Here, the integration over ϕ_κ can be done analytically with the result 2π, since $T_{if}^+(\boldsymbol{\eta})$ [and, hence, $Q_{if}^+(\boldsymbol{\kappa})$] does not depend upon ϕ_κ. However, the integrations over κ and θ_κ have to be carried out numerically. Hence, according to the BDW-4B method, the total cross section is derived in terms of a five-dimensional numerical quadrature over real variables. The main features of these numerical integrations, including the Cauchy regularization of the quadrature over variable t_1, are given in the Appendix.

TABLE I. Total cross sections Q_{if}^+ in the BDW-4B method as a function of the laboratory impact energy E for transfer ionization $H^+ + {}^4He \longrightarrow H + {}^4He^{2+} + e$. The numbers in square brackets denote powers of 10, e.g., 7.88[−21] ≡ 7.88 × 10^{-21}.

E (MeV)	0.3	0.4	0.5	0.75	1
Q_{if}^+ (cm^2)	7.88[−21]	3.09[−21]	1.32[−21]	2.30[−22]	5.90[−23]
E (MeV)	1.5	2	5	7.5	10
Q_{if}^+ (cm^2)	7.72[−24]	1.73[−24]	1.26[−26]	1.37[−27]	2.79[−28]

III. RESULTS AND DISCUSSION

As an illustration of the BDW-4B method for transfer ionization, the following prototype collision between proton and helium is investigated:

$$ H^+ + He \longrightarrow H + He^{2+} + e, \quad (19)$$

with $Z_P = 1$ and $Z_T = 2$. The results from the present computations of total cross sections for process (19), at impact energies E = 0.3–10 MeV, are given in Table I, as well as in Fig. 1. As can be seen from Fig. 1, the BDW-4B method underestimates the experimental data [5,7,9] at energies 0.3−3 MeV. On the other hand, the agreement between the theory and the measurement [9] is very good at impact energies larger than 3 MeV. Based upon the earlier experience with transfer ionization treated by the CDW-4B method [19,20], it is anticipated that the explicit inclusion of the presently omitted dynamic electron correlation effects would improve the overall standing of the BDW-4B theory with respect to all the existing experimental data at intermediate-to-high energies. The results on this will be reported shortly.

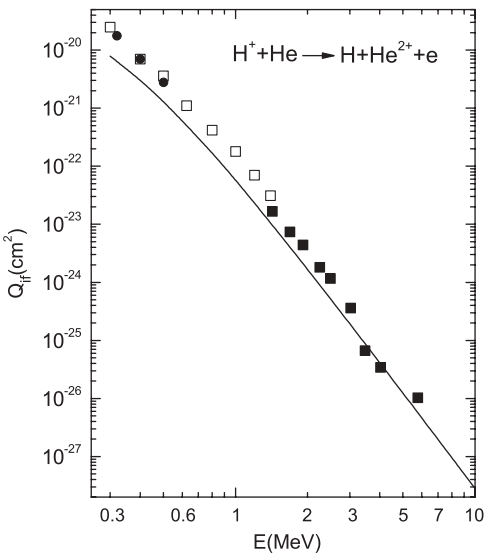

FIG. 1. Total cross sections Q_{if} as a function of the laboratory impact energy E for transfer ionization $H^+ + {}^4He \longrightarrow H + {}^4He^{2+} + e$. Theory: the post form of the BDW-4B method (solid line: present, $Q_{if} \equiv Q_{if}^+$). Experimental data: • Shah and Gilbody [5], □ Mergel *et al.* [7], and ■ Schmidt *et al.* [9].

IV. CONCLUSION

We have investigated the problem of transfer ionization in collisions between bare ions and two-electron atomic systems. A second-order theory termed the four-body Born distorted wave (BDW-4B) method is formulated and implemented. The scattering wave functions of the proposed method exhibit the correct asymptotic behaviors in both the entrance and exit channels, which was the objective of the Dollard asymptotic convergence problem for atomic collisions with the presence of Coulomb potentials at infinitely large separations between the scattering aggregates. The BDW-4B theory is illustrated by its application to transfer ionization in H^+-He collisions at impact energies $E = 0.3$–10 MeV. Agreement of the obtained theoretical total cross sections with the available experimental data is especially good at larger energies.

ACKNOWLEDGMENTS

Dž. Belkić acknowledges support by the Swedish King Gustav the 5th Jubilee Foundation and the Swedish Cancer Society Research Fund. I. Mančev acknowledges support by the Ministry of Science of the Republic of Serbia through Project Nr. 171020.

APPENDIX

Integral $\mathcal{F}_1(\boldsymbol{R})$ from Eq. (15) can be analytically reduced to a one-dimensional integral following Ref. [38] with the final result

$$\mathcal{F}_1(\boldsymbol{R}) = 2\pi Z_P t_1 \omega e^{i\alpha\cdot R}\int_0^1 dt \frac{t(1-t)e^{-i\boldsymbol{Q}_1\cdot\boldsymbol{R}-\Delta_1 R}}{\Delta_1^5} \times [a_1 R^2 - b_1 R - c_1 - d_1(1+\Delta_1 R)\boldsymbol{R}\cdot\hat{\boldsymbol{v}}], \quad \text{(A1)}$$

where

$$\boldsymbol{Q}_1 = \boldsymbol{\alpha} t - \boldsymbol{\beta}_1(1-t), \quad \Delta_1^2 = v_1^2 t(1-t) + Z_P^2 t + \lambda_1^2(1-t), \quad \text{(A2)}$$

$$\boldsymbol{\beta}_1 = \boldsymbol{\beta} + \boldsymbol{v}t_1, \quad \boldsymbol{v}_1 = \boldsymbol{v}(1-t_1), \quad \lambda_1 = b - \omega t_1, \quad a_1 = \Delta_1^2\delta_1^+, \quad b_1 = c_1\Delta_1, \quad \text{(A3)}$$

$$\omega = iv, \quad \delta_1 = \lambda_1 - \gamma_1, \quad \gamma_1 = \omega t(1-t_1), \quad \text{(A4)}$$

$$c_1 = 3\delta_1^-, \quad \delta_1^\pm = \Delta_1^2 \pm \gamma_1'\delta_1, \quad d_1 = -\Delta_1^2(\gamma_1' + \delta_1), \quad \gamma_1' = \omega(1-t)(1-t_1). \quad \text{(A5)}$$

On the other hand, the integral $\mathcal{D}_2$ from Eq. (12) can be analytically calculated by means of the complex contour technique of Nordsieck [51] so that

$$\mathcal{D}_2 = \frac{8\pi}{\kappa^2+b^2} T_0^{i\zeta}\mathcal{R}_0, \quad \text{(A6)}$$

where

$$T_0^{-1} = 1 - 2\frac{\boldsymbol{\kappa}\cdot\boldsymbol{p} + ibp}{\kappa^2+b^2}, \quad \mathcal{R}_0 = b\frac{1-i\zeta}{\kappa^2+b^2} + i\zeta\frac{b-ip}{\kappa^2+b^2-2\boldsymbol{\kappa}\cdot\boldsymbol{p}-2ibp}. \quad \text{(A7)}$$

In this way, the expression for the transition amplitude in Eq. (10) reads

$$T_{if}^+ = \frac{16N^{-*}Z_P^{5/2}N_b^2\pi^{3/2}\omega}{\Gamma(i\nu_T)\Gamma(1-i\nu_T)}\frac{T_0^{i\zeta}\mathcal{R}_0}{\kappa^2+b^2} \times \int_0^1 dt_1 f_T(t_1)t_1\int_0^1 dt\frac{t(1-t)}{\Delta_1^5}J(t_1), \quad \text{(A8)}$$

$$J(t_1) = a_1 I_3 - b_1 I_2 - c_1 I_1 + \frac{d_1}{\omega}(K_1 + \Delta_1 K_2), \quad \text{(A9)}$$

where

$$I_n = \int d\boldsymbol{R} R^{n-1}(vR + \boldsymbol{v}\cdot\boldsymbol{R})^{i\xi}e^{-i\boldsymbol{Q}_1\cdot\boldsymbol{R}-\Delta_1 R}, \quad (n = 1,2,3), \quad K_n = \boldsymbol{v}\cdot\nabla_{Q_1} I_n. \quad \text{(A10)}$$

Integrals $I_{1,2,3}$ and, consequently, $K_{1,2}$ can also be analytically calculated along the lines in Ref. [38], and the following result is obtained for $J(t_1)$:

$$J(t_1) = 8\pi\Gamma(1+i\xi)\mathcal{F}D(\mathcal{A} - i\xi\mathcal{B}), \quad \text{(A11)}$$

where

$$\mathcal{A} = -2a_1\frac{D}{\Delta_1}A_\beta + \frac{b_1}{\Delta_1}A_\alpha - c_1 - 2\frac{d_1 D}{\omega\Delta_1}(A_1 - A_2), \quad \text{(A12)}$$

$$\mathcal{B} = 2a_1\frac{D}{\Delta_1}B_\beta - \frac{b_1}{\Delta_1}B_\alpha - c_1 C + 2\frac{d_1 D}{\omega\Delta_1}(B_1 - B_2), \quad \text{(A13)}$$

$$\mathcal{F} = \frac{B^{i\xi}}{Q_1^2+\Delta_1^2}, \quad B = \frac{2(v\Delta_1 - i\boldsymbol{Q}_1\cdot\boldsymbol{v})}{Q_1^2+\Delta_1^2}, \quad \text{(A14)}$$

$$C = \frac{v}{B\Delta_1} - 1, \quad A = \frac{\Delta_1^2}{Q_1^2+\Delta_1^2}, \quad D = \frac{A}{\Delta_1}, \quad \text{(A15)}$$

$$A_\alpha = 1 - 4A, \quad B_\alpha = 1 + 2AC_\alpha, \quad C_\alpha = C[4 + (1-i\xi)C], \quad \text{(A16)}$$

$$A_\beta = 6(1-2A), \quad B_\beta = 2AC_\beta + 3D_\beta, \quad \text{(A17)}$$

$$C_\beta = C[18 + 9(1-i\xi)C + (1-i\xi)(2-i\xi)C^2], \quad D_\beta = 2 - (1+i\xi)C, \quad \text{(A18)}$$

$$A_1 = \{2 + i\xi[2 - (1+i\xi)C]\}, \quad B_1 = u\omega[2 + (1-i\xi)C], \quad \text{(A19)}$$

$$A_2 = \{2(1-6A) + i\xi[2AC_2 + (3+i\xi)]\}(\boldsymbol{Q}_1\cdot\boldsymbol{v}), \quad C_2 = (1+i\xi)C[6 + (1-i\xi)C] - 6, \quad B_2 = u\omega[(1+i\xi) - 2AC_2'], \quad \text{(A20)}$$

$$C_2' = (1-i\xi)C[6 + (2-i\xi)C] + 6, \quad u = (1+C)\Delta_1. \quad \text{(A21)}$$

Therefore, this derivation reduces the nine-dimensional integration for the matrix element T_{if}^+ from Eq. (10) to a two-dimensional numerical quadrature over the real variables $\{t_1, t\}$.

We made use of the Gauss-Legendre quadrature rule for the numerical integrations over κ, θ_κ, and η in Eqs. (17) and (18). To this end, it is convenient to introduce the change of variables according to $\kappa = \sqrt{2(1+x)/(1-x)}$, $x \in [-1,+1]$, $\cos\theta_\kappa = u$, $u \in [-1,+1]$, $\eta = \sqrt{2(1+y)/(1-y)}$, and $y \in [-1,+1]$. The latter change of variable in η is

very important, since it concentrates the integration points near the forward cone [52], which gives the dominant contributions because of the eikonal nature of scattering for heavy projectiles. The singularities at $x = 1$ and $y = 1$ are superficial, as they disappear after a full analytical scaling of the integrand. By this scaling, the only place where the inverses $1/(1-x)$ and $1/(1-y)$ appear in $|T_{if}^{+}(\boldsymbol{\eta})|^2$ is through the overall multiplicative term $S \equiv \sqrt{1-x}\,|(1-x)^{9/2+i\xi}(1-y)^{1+i\xi}|^2$. Finally, the product of S with the differentials $\kappa^2 d\kappa\, \eta d\eta$ yields $4\sqrt{2(1+x)}(1-x)^7 dx\, dy$, so that all the integrands in Eqs. (16)–(18) are regular functions at $x = 1$ and $y = 1$.

Special attention has to be paid to the integration over t_1. Namely, this quadrature requires a numerical computation of an integral of the type

$$I = \frac{1}{B(i\nu_{\mathrm{T}}, 1-i\nu_{\mathrm{T}})} \int_0^1 dt_1 t_1^{i\nu_{\mathrm{T}}-1}(1-t_1)^{-i\nu_{\mathrm{T}}} f(t_1), \quad \text{(A22)}$$

where $B(i\nu_{\mathrm{T}}, 1-i\nu_{\mathrm{T}})$ is the beta function [50] and $f(t_1)$ is regular in the considered interval [0, 1]. Here, the integrand possesses integrable branch-point singularities at $t_1 = 0$ and $t_1 = 1$. Following Ref. [53], we apply the Cauchy regularization of the whole integrand. With this goal in mind, we first conveniently rewrite the expression for I as

$$I = \frac{1}{B(i\nu_{\mathrm{T}}, 1-i\nu_{\mathrm{T}})} \left\{ \int_0^1 dt_1 \left(\frac{t_1}{1-t_1}\right)^{i\nu_{\mathrm{T}}} \frac{f(t_1) - t_1 f_{1,0} - f(0)}{t_1} + f_{1,0} \int_0^1 dt_1 \left(\frac{t_1}{1-t_1}\right)^{i\nu_{\mathrm{T}}} + f(0) \int_0^1 dt_1 \left(\frac{t_1}{1-t_1}\right)^{i\nu_{\mathrm{T}}} \frac{1}{t_1} \right\}, \quad \text{(A23)}$$

where $f_{1,0} = f(1) - f(0)$. This is followed by the simultaneous Cauchy regularization of both branch-points singularities at $t_1 = 0$ and $t_1 = 1$:

$$I = \frac{i\sinh(\pi\nu_{\mathrm{T}})}{\pi} \int_0^1 dt_1 \left(\frac{t_1}{1-t_1}\right)^{i\nu_{\mathrm{T}}} \frac{f(t_1) - t_1 f_{1,0} - f(0)}{t_1} + i\nu_{\mathrm{T}} f_{1,0} + f(0), \quad \text{(A24)}$$

where we have utilized the well-known properties of the beta and gamma functions [50]. In this way, the regularized integration over t_1 in Eq. (A24) becomes well adapted for the application of the Gauss-Legendre numerical quadrature. Another procedure which is also employed in our algorithm consists of splitting the interval [0,1] into two sub-intervals: (i) [0, 1/2] and (ii) [1/2,1]. This is followed by changing the integration variable as in Ref. [54] via $t_1 = (1/2)e^{-w}$ for [0, 1/2] and $t_1 = 1 - (1/2)e^{-w}$ for [1/2,1], so that the integral from Eq. (A24) is reduced to the form $\int_0^\infty dw[f_1(w) + f_2(w)]e^{-w}$, which can be evaluated by using the Gauss-Laguerre quadrature method. Both procedures are found to yield the same numerical results.

As a test of the numerical integration over κ in $\int_0^\infty d\kappa\, g(\kappa)$, instead of the change of the variable $\kappa = \sqrt{2(1+x)/(1-x)}$, we also used the substitution $\kappa = \tan(\pi[x+1]/4)$:

$$\int_0^\infty d\kappa\, g(\kappa) = \int_{-1}^1 dx\, g\{\tan(\pi[x+1]/4)\} \frac{\pi}{4} \sec^2(\pi[x+1]/4). \quad \text{(A25)}$$

Then, the Gauss-Legendre quadrature is applied to the right-hand side of Eq. (A25) and the same numerical results are obtained. Likewise, we also applied the Gauss-Laguerre quadrature for integration over κ and arrived at the same numerical results. The number of integration points for each axis is gradually and systematically increased until convergence to the preassigned two decimal places has reliably been reached.

[1] Dž. Belkić, *Quantum Theory of High-Energy Ion-Atom Collisions* (Taylor & Francis, London, 2008).
[2] Dž. Belkić, I. Mančev, and J. Hanssen, Rev. Mod. Phys. **80**, 249 (2008).
[3] Dž. Belkić, J. Math. Chem. **47**, 1420 (2010).
[4] J. McGuire, *Electron Correlation Dynamics in Atomic Collisions* (Cambridge University Press, Cambridge, 1997).
[5] M. B. Shah and H. B. Gilbody, J. Phys. B: At. Mol. Phys. **18**, 899 (1985).
[6] M. B. Shah, P. McCallion, and H. B. Gilbody, J. Phys. B: At. Mol. Opt. Phys. **22**, 3037 (1989).
[7] V. Mergel *et al.*, Phys. Rev. Lett. **79**, 387 (1997).
[8] H. T. Schmidt *et al.*, Phys. Rev. Lett. **89**, 163201 (2002).
[9] H. T. Schmidt *et al.*, Phys. Rev. A **72**, 012713 (2005).
[10] H. T. Schmidt, A. Fardi, J. Jensen, P. Reinhed, R. Schuch, K. Støchkel, H. Zettergren, H. Cederquist, and L. Cocke, Nucl. Instr. Meth. Phys. Res. B **233**, 43 (2005).
[11] O. Woitke, P. A. Závodszky, S. M. Ferguson, J. H. Houck, and J. A. Tanis, Phys. Rev. A **57**, 2692 (1998).
[12] M. M. Sant'Anna, A. C. Santos, L. F. Coelho, G. Jalbert, N. V. de Castro Faria, F. Zappa, P. Focke, and Dž. Belkić, Phys. Rev. A **80**, 042707 (2009).
[13] K. M. Dunseath and D. S. F. Crothers, J. Phys. B: At. Mol. Opt. Phys. **24**, 5003 (1991).
[14] R. Shingal and C. D. Lin, J. Phys. B: At. Mol. Opt. Phys. **24**, 251 (1991).
[15] R. Gayet and A. Salin, J. Phys. B: At. Mol. Phys. **20**, L571 (1987).

[16] B. W. Ding, D. Y. Yu, and X. M. Chen, Nucl. Instr. Meth. Phys. Res. B **266**, 886 (2008).
[17] M. E. Galassi, P. N. Abufager, A. E. Martinez, R. D. Rivarola, and P. D. Fainstein, J. Phys. B: At. Mol. Opt. Phys. **35**, 1727 (2002).
[18] A. L. Godunov, J. H. McGuire, V. S. Schipakov, H. R. J. Walters, and C. T. Whelan, J. Phys. B: At. Mol. Opt. Phys. **39**, 987 (2006).
[19] Dž. Belkić, I. Mančev, and V. Mergel, Phys. Rev. A **55**, 378 (1997).
[20] I. Mančev, Phys. Rev. A **64**, 012708 (2001).
[21] J. Pálinkás, R. Schuch, H. Cederquist, and O. Gustafsson, Phys. Rev. Lett. **63**, 2464 (1989); Phys. Scr. **42**, 175 (1990).
[22] J. Briggs and K. Taulbjerg, J. Phys. B: At. Mol. Phys. **12**, 2565 (1979).
[23] T. Ishihara and J. H. McGuire, Phys. Rev. A **38**, 3310 (1988).
[24] S. G. Tolmanov and J. H. McGuire, Phys. Rev. A **62**, 032711 (2000).
[25] G. Bernardi, P. Focke, A. D. Gonzalez, S. Suarez, and D. Fregenal, J. Phys. B: At. Mol. Opt. Phys. **32**, L451 (1999).
[26] L. Sarkadi, L. Lugosi, K. Tőkési, L. Gulyás, and Á. Kövér, J. Phys. B: At. Mol. Opt. Phys. **34**, 4901 (2001).
[27] A. L. Godunov, C. T. Whelan, and H. R. J. Walters, J. Phys. B: At. Mol. Opt. Phys. **37**, L201 (2004).
[28] A. L. Godunov *et al.*, Phys. Rev. A **71**, 052712 (2005).
[29] M. S. Schöffler *et al.*, J. Phys. B: At. Mol. Opt. Phys. **38**, L123 (2005).
[30] A. L. Godunov, C. T. Whelan, and H. R. J. Walters, Phys. Rev. A **78**, 012714 (2008).
[31] A. B. Voitkiv, J. Phys. B: At. Mol. Opt. Phys. **41**, 195201 (2008).
[32] Yu. V. Popov, O. Chuluunbaatar, S. I. Vinitsky, L. U. Ancarani, C. Dal Cappello, and P. S. Vinitsky, JETP **95**, 620 (2002).
[33] S. Houamer, Yu. V. Popov, and C. Dal Cappello, Phys. Rev. A **81**, 032703 (2010).
[34] V. Mergel, R. Dörner, Kh. Khayyat, M. Achler, T. Weber, O. Jagutzki, H. J. Lüde, C. L. Cocke, and H. Schmidt-Böcking, Phys. Rev. Lett. **86**, 2257 (2001).
[35] H. Schmidt-Böcking *et al.*, Europhys. Lett. **62**, 477 (2003).
[36] F. Afaneh, R. Dörner, L. Schmidt, Th. Weber, K. E. Stiebing, O. Jagutzki, and H. Schmidt-Böcking, J. Phys. B: At. Mol. Opt. Phys. **35**, L229 (2002).
[37] S. Martínez, G. Bernardi, P. Focke, S. Suárez, and D. Fregenal, J. Phys. B: At. Mol. Opt. Phys. **41**, 145204 (2008).
[38] Dž. Belkić, Nucl. Instr. Meth. Phys. Res. B **86**, 62 (1994).
[39] Dž. Belkić, I. Mančev, and M. Mudrinić, Phys. Rev. A **49**, 3646 (1994).
[40] Dž. Belkić, *Principles of Quantum Scattering Theory*, Series in Atomic and Molecular Physics (Institute of Physics, Bristol, 2004).
[41] J. D. Dollard, J. Math. Phys. **5**, 729 (1964).
[42] I. M. Cheshire, Proc. Phys. Soc. **84**, 89 (1964).
[43] Dž. Belkić, R. Gayet, and A. Salin, Phys. Rep. **56**, 279 (1979).
[44] Dž. Belkić, J. Phys. B: At. Mol. Opt. Phys. **26**, 497 (1993).
[45] I. Mančev, J. Phys. B: At. Mol. Opt. Phys. **36**, 93 (2003).
[46] I. Mančev, Europhys. Lett. **69**, 200 (2005).
[47] I. Mančev, J. Comp. Methods Sci. Eng. **5**, 73 (2005).
[48] Dž. Belkić, J. Math. Chem. **47**, 1366 (2010).
[49] E. Hylleraas, Z. Phys. **54**, 347 (1929).
[50] I. S. Gradshteyn and I. M. Ryzhik, *Tables of Integrals, Series and Products*, 6th ed. (Academic Press, New York, 2000).
[51] A. Nordsieck, Phys. Rev. **93**, 785 (1954).
[52] Dž. Belkić, Phys. Rev. A **37**, 55 (1988).
[53] Dž. Belkić, Phys. Rev. A **47**, 3824 (1993).
[54] S. C. Mukherjee, K. Roy, and N. C. Sil, Phys. Rev. A **12**, 1719 (1975).